

Performance Analysis for 5G/6G Satellite Communication under Nonlinear HPA Channel

Pansoo Kim, Joon-Gyu Ryu and Seungkeun Park

Radio & Satellite Research Division, ETRI

Daejeon, Republic of Korea

pskim@etri.re.kr, jgryurt@etri.re.kr, seungkp@etri.re.kr

Abstract — In this paper, we have presented the performance results of NR-compliant waveforms under nonlinear HPA channels which also can be candidates for B5G/6G satellite communication for integrated terrestrial and satellite networks.

Keywords— B5G/6G satellite communication, Nonlinear HPA, CP-OFDM, NTN

I. INTRODUCTION

Recently, the integration of terrestrial networks (TN) and non-terrestrial networks (NTN) has drawn great interest in the third-generation partnership project (3GPP) for the beyond 5G (B5G) and 6G standards [1]. It would be desirable to unify the air interface between two different networks from the several system requirements point of view [2][3]. Prior to the substantial work for 5G NTN networks, there were extensive studies about new waveforms for New Radio (NR) system. Apart from the selected CP-OFDM and DFT-s-OFDM schemes used in the LTE, Filtered OFDM (f-OFDM), Windowed OFDM (W-OFDM), Filter Bank Multicarrier (FBMC), Universal Filtered Multicarrier (UFMC), and Generalized Frequency Division Multiplexing (GFDM) were proposed and analyzed [4]. For the TN networks scenario, the proposed waveforms have improved lower Out-Of-Band-Emissions (OOBE) characteristics but mostly are still characterized as high Peak to Average Power Ratio (PAPR) signals. The NTN network is recognized as power limited system due to a large path loss by long propagation between gNB and UE. Thus, to secure more signal power gain, its operation should be close to the saturated region from the high power amplifier (HPA) which appears to nonlinear effect. Consequently, a pre-distortion scheme to overcome nonlinear amplifier characteristics can be typically used to reduce signal impairments in the ground segment. In this paper, we have presented the performance results under nonlinear HPA when NR-compliant waveforms are used. The paper is organized as follows. In the next section, we describe the system model. For comparative performance analysis, the simulation results are presented in section III.

II. SYSTEM MODEL

The OFDM signal $s(m)$ can be represented as

$$s(m) = \sum_n \sum_{k=0}^{N-1} d_k(n) p(m - nN) \exp j\{2\pi k(m - nN)\Delta_f\} \quad (1)$$

where n is the symbol index and k is the subcarrier index, respectively. The $d_k(n)$ denotes I/Q signal in the time/frequency

domain, $p(n)$ prototype filter impulse response, Δ_f carrier spacing, and N is the number of active subcarriers. As mentioned, OOBE can generally be further reduced by passing the signal through a pass-band filter $f(n)$.

$$y(n) = s(n) * f(n) \quad (2)$$

where $*$ is the linear convolution operator. The different waveforms are optimized through the selection and design of the two filters $p(n)$ and $f(n)$. The function of $p(n)$ windowing and $f(n)$ filtering is denoted as W-OFDM and f-OFDM transmission respectively. In this paper, we mainly refer to [5] and [6] for windowing and filtering schemes.

For HPA model, we have considered two kinds of general channel models consisting of an ideal linearized HPA acting as a hard limiter to amplitude variation and a realistic one. The ideal limiter model AM/AM can be expressed as

$$y(t) = \begin{cases} \frac{y_{sat}}{x_{sat}} x(t) & \text{for } |x(t)| < x_{sat} \\ y_{sat} & \text{for } |x(t)| \geq x_{sat} \end{cases} \quad (3)$$

where $x(t)$ and $y(t)$ are the input and output signals from the ideal limiter, respectively; x_{sat} and y_{sat} are the input and output saturation (clipping) levels. The realistic channel model based on the measurement is shown in Fig. 1.

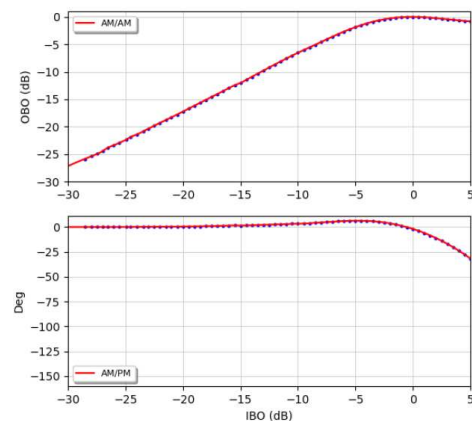


Figure 1. HPA AM/AM and AM/PM model

III. PERFORMANCE COMPARISON AND ANALYSIS

A. PAPR comparison

The PAPR of the signal can be expressed as

$$\lambda = \frac{\max\{|x_n|^2, 0 \leq n < N\}}{\frac{1}{N} \sum_{n=0}^{N-1} |x_n|^2} \quad (4)$$

where x_n are independent and identically distributed with Gaussian complex distribution Nyquist rate samples and N is the number of samples. The CCDF is as follows

$$CCDF(\lambda) = 1 - \prod_{n=0}^{N-1} \Pr\left(\frac{|x_n|^2}{\sigma^2} \leq \lambda\right) = 1 - (1 - e^{-\lambda})^N \quad (5)$$

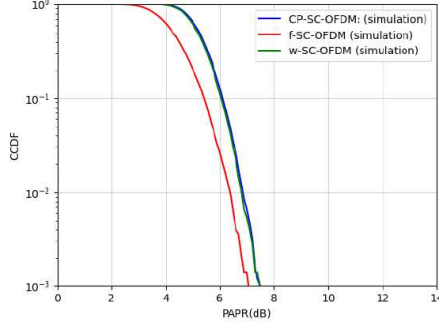
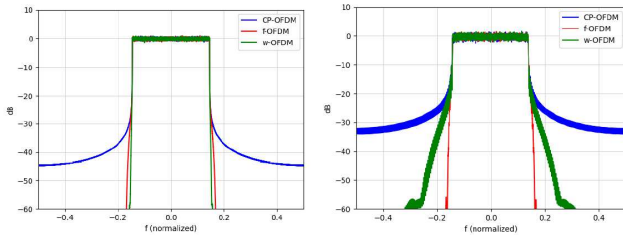


Figure 2. PAPR performance of DFT-s-OFDM scheme with filtering/widowing function when subcarrier spacing 240kHz

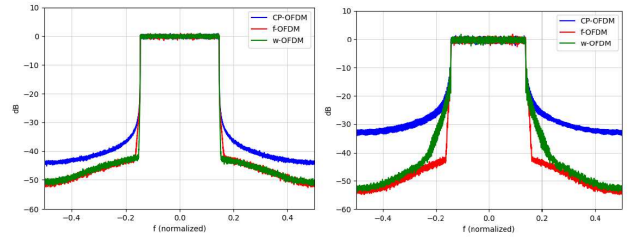
As shown in Fig. 2, the f-SC-OFDM (filtered single carrier OFDM, DFT-s-OFDM) seems to be slightly better than w-SC-OFDM (windowed single carrier OFDM) and CP-SC-OFDM (Cyclic Prefix single carrier OFDM) in terms of PAPR performance.

B. Power Spectral Density (PSD) measurements

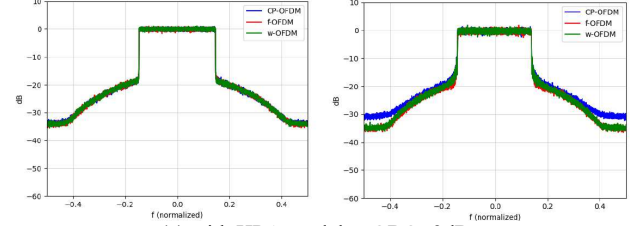
As depicted in Fig. 3(a), OOB performance is significantly improved with f-OFDM and w-OFDM but the improvement would disappear when the HPA nonlinear channel is incorporated even though the perfect pre-distortion scheme is applied in Fig. 3 (c)(d). This is caused by the PAPR characteristics of these signals and is similar even when DFT precoding is used. When Input Back Off (IBO) is very significantly increased from Output Back Off (OBO) -3dB to OBO -8dB so that most of the input signal works in the linear part of the amplifier characteristic, then f-OFDM and w-OFDM are better than CP-OFDM in terms of OOB like Fig. 3(b).



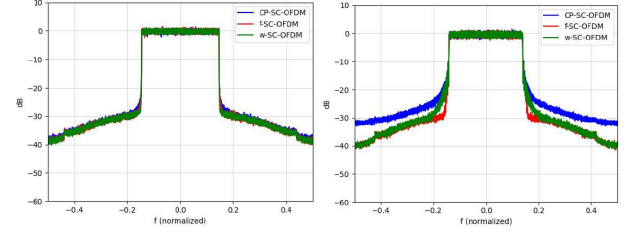
(a) without HPA model
(left: subcarrier spacing 15kHz, right: subcarrier spacing 240kHz)



(b) with HPA model at OBO -8dB
(left: subcarrier spacing 15kHz, right: subcarrier spacing 240kHz)



(c) with HPA model at OBO -3dB
(left: subcarrier spacing 15kHz, right: subcarrier spacing 240kHz)



(d) with HPA model at OBO -3dB and DFT precoding
(left: subcarrier spacing 15kHz, right: subcarrier spacing 240kHz)

Figure 3. PSD measurements

Acknowledgement

This work was supported by Institute of Information & communications Technology Planning & Evaluation (IITP) grant funded by the Korea government (MSIT) (No.2021-0-00847, Development of 3D Spatial Satellite Communications Technology).

References

- [1] 3GPP TR 38.811 - V15.1.0 (2019-06) – “Study on New Radio (NR) to support non-terrestrial networks (Release 15)”
- [2] A. Jayaprakash *et al.*, “New Radio Numerology and Waveform Evaluation for Satellite Integration into 5G Terrestrial Network,” in *Proc. IEEE Int'l. Conf. Commun. (ICC)*, May, 2020, pp. 1–7.
- [3] A. Jayaprakash *et al.*, “Analysis of candidate waveforms for integrated satellite-terrestrial 5g systems,” in *Proc. IEEE 2nd 5G World Forum (5GWF)*, 2019, pp. 636–641.
- [4] M. Elkourdi, B. Pekoz, E. Guvenkaya and H. Arslan, “Waveform design principles for 5G and beyond,” in *Proc. IEEE 17th Annu. Wireless Microw. Technol. Conf.*, 2016, pp. 1-6.
- [5] R. Zayani, Y. Medjahdi, H. Shaiek, and D. Roviras, “WOLA-OFDM: A potential candidate for asynchronous 5G,” in *proc. IEEE Globecom Workshops (GC Wkshps)*, Dec. 2016, pp. 1–5.
- [6] X. Zhang, L. Zhang, P. Xiao, D. Ma, J. Wei, and Y. Xin, “Mixed numerologies interference analysis and inter-numerology interference cancellation for windowed OFDM systems,” *IEEE Trans. on Vehicular Technol.*, vol. 67, no. 8, pp. 7047–7061, Aug. 2018